Ions in crystals: The topology of the electron density in ionic materials. I. Fundamentals

A. Martín Pendás, Aurora Costales, and Víctor Luaña
Departamento de Química Física y Analítica, Facultad de Química,
Universidad de Oviedo, E-33006 Oviedo, Spain
(Received 14 December 1995)

The topological theory of atoms in molecules is applied to periodic crystalline ionic systems. A systematic investigation of the fundamental properties of the topology of the charge density in crystals is undertaken, and several basic facts, peculiar to the solid state and not previously explored, to our knowledge, are put forward. We also show how the theory allows us to define unambiguously very important concepts of solid-state theory, like the coordination index or the coordination polyhedron of an ion in a solid. We particularize our results by means of the detailed study of an example crystal, the rocksalt phase of LiI. It is shown that this crystal is best described as made up of 18-fold-coordinated iodides and sixfold-coordinated lithiums, contrary to the usual six-six description. [S0163-1829(97)09304-1]

I. INTRODUCTION

A large part of our chemical and physical wisdom is based on the concept of interacting atoms or ions that mostly maintain their individuality when transferred among different compounds, and that confer well-defined properties to materials. Quantum-mechanical pictures of isolated molecules or condensed phases, however, have traditionally been much less prone to such prevalent images of the chemical world, giving rise to the longly debated problem of how to recover atomic, ionic, or group behavior from quantum descriptions. So deeply rooted for the chemist or physicist is the need to partition physically every global system property into isolated contributions, that over the years hundreds of different recipes or models to perform this task have appeared in the literature. Of paramount importance is the fact that most modern theories of bonding are based, in one way or another, on the partition of charge (or electronic density) among the different nuclear centers under study, usually by means of Mulliken—i.e., projected density of states in solids—analyses. In this way, an important amount of the interpretative models of chemical behavior are based on concepts that are known to be very badly defined, and to give answers extremely dependent on a whole hierarchy of approximations. As an example, Mulliken populations depend on the concept of orbital, and are therefore nonobjective functions of the computational method used to obtain them.

It should be clear from the preceding paragraph that any attempt to construct a firm theory of bonding that allows us to recover the empirical concept of an atom in a molecule must be based on a quantum mechanically well-defined partition of physical space. In this way, the topological properties of observables become central to the treatment. The importance of the topology of several scalar fields in chemistry has been repeatedly put forward in recent years.[1] Different definitions of the basic topological space and its sets give rise to different and complementary schemes. However, if we expect to recover the observed additivity of group properties from our treatment, we are advocated to consider a topology that allows the generalizaton of quantum mechanics to open systems. Such a theory has been constructed by Bader,[2] considering the topology of the electron density. Over the years it has proven to provide a sound foundation to some of the most important phenomenological models of chemical bonding, like the valence shell electron pair repulsion model,[3] an improved version of the historical Lewis pair model. It has also shown how quantum-mechanical electron densities calculated at different approximation levels can be used to recover group or bond properties in excellent agreement with experiment.[4]

Unfortunately, Bader's own background has conditioned its diffusion stream mainly to molecular quantum chemistry, and the theory has not achieved in condensed phases the development status found in molecular systems. There are good reasons, nevertheless, to undertake such a research in the solid state. On the one hand, translational symmetry, as opposed to rotational symmetry in the molecular environment, imposes severe restrictions on the type and number of critical points that a periodic scalar function, like the electron density, may show. Moreover, the toroidal, boundless nature of the physical space, in which atoms are embedded in a perfectly periodic crystal, makes it necessary that the volume associated with a given group of atoms remains finite. This situation is extremely unusual in an isolated molecule, and allows us to define geometrical concepts—i.e., atomic or group radii, group volumes, etc.—that, being necessarily ill defined in normal molecules, may now be compared and correlated with a vast amount of empirical or semiempirical data. On the other hand, the connection between the adiabatic electronic energy surface of the crystal ground state and its static thermodynamics opens the way to a study of the behavior of bonding properties with pressure and temperature.

Through the years, several authors, including Bader himself, have applied these ideas to crystalline solids, uncovering many important facts about the topological features of the electron density in periodic systems. Some of these studies, particularly those of Eberhart and co-workers,[5] focused on metallic alloys, and have revealed interesting connections among macroscopic properties, like bulk moduli and electron densities. Other ones, mainly addressed by Bader and co-workers,[6] showed some of the formal features and basic

 © 1997 The American Physical Society

shapes of electron densities in crystals that arise from the periodicity of space.

A systematic study of the complete topology of the electron density in a periodic solid seems to be lacking. In this work we will try to establish the main characteristics of the topology of the electronic density in these systems. Our focus will be addressed more toward the less-known interatomic or intermolecular features than to the now well-understood intramolecular ones.[2] Simple ionic systems seem well suited for these purposes. The whole topological picture is interionic in nature here. Moreover, the very concept of atomic radii was born when systematizing the x-ray lattice parameters obtained for the alkali halides. We have chosen perovskites and alkali halides as a starting point. Despite their extreme structural simplicity, we will show how they hide a rich number of different topological structures that evolve following purely geometrical criteria.

In this first paper we will present Bader's theory in the context of a periodic system, together with a detailed study of the topological properties of a prototypical alkali halide. The second paper will present an application of the general scheme presented here to the slightly more complex perovskite structure compounds. A third paper in the series will be devoted to an analysis of the geometrical trends emerging from a systematic study of the topology of the charge density in the rocksalt phase of alkali halides. Finally, a fourth paper will address the relation between topological and energetic properties, particularized to the case of the pressure-induced $B1$ (rocksalt) to $B2$ (cesium chloride) phase transition of the alkali halides, for which a detailed *ab initio* study has previously been reported.[7]

The rest of the paper is organized as follows: In Section II we will introduce Bader's theory, stating its main points and the usual terminology associated with it. We will then study those features of the theory to be found only in the solid state, as well as the computational implementation of an original and efficient automatic procedure able to extract the whole topology of a crystal without human intervention. Sec. III is devoted to a study of the topological picture of a prototypic alkali halide, the lithium iodide, in its rocksalt phase. Finally, we will give some conclusions and prospects in Sec. IV.

II. FUNDAMENTALS

A. Bader's atoms in molecules theory

Here we will provide a minimal set of the main results of the topological theory of atoms in molecules. A full, authoritative account of the theory may be found in Refs. 2 and 8, and in the works cited therein. Our treatment closely follows that found in Ref. 8.

It may be proven that in order to obtain a well-behaved quantum-mechanical description of an open region of a quantum system, the region must be bounded by a surface whose flux of the gradient of the electron density vanishes. Let us denote by the symbol Ω an open three-dimensional region in the physical space, and by S or S_Ω its bidimensional boundary. The previous condition is written as

$$\nabla\rho\cdot\mathbf{n}=0 \tag{1}$$

for every point in S_Ω, $\mathbf{n}$ being the exterior normal vector to the boundary surface.

The most important topological property of the charge density of an electronic system is the presence of maxima at the nuclear positions. Equation (1) allows us actually to partition the physical space into nonoverlapping regions that, in general, contain only one nucleus. In order to obtain a more clear picture of the appearance of those regions, a few comments regarding the general features of the charge density gradient vector field ($\nabla\rho$) are due. Every field line or trajectory of the field, thought of as creating a dynamical system, has its origin ($t\rightarrow-\infty$, α–limit) and its end ($t\rightarrow\infty$, ω–limit, attractor) at critical points, $\nabla\rho=\vec{0}$. Clearly, an enumeration and classification of the critical points of the field is an important step toward the topological identification of the field. Four nondegenerate kinds of critical points are possible in three dimensions: maxima, minima, first-kind saddle points, and second-kind saddle points. Following Bader's notation, we classify them according to the (*rank, signature*) convention. The rank is defined as the number of nonzero eigenvalues of the Hessian matrix of the charge density. The signature being the algebraic sum of the signs of the eigenvalues. Although the nuclei of a system introduce a cusp in the electronic density, nuclei are topologically identical to maxima or $(3,-3)$ critical points. Very few examples of nonnuclear maxima have been found up to now. The other types of critical points are usually named with terms whose meaning will soon turn clear: $(3,-1)$ or bond point, $(3,+1)$ or ring point, and $(3,+3)$ or cage point. The set of points sharing a given ω limit is usually called the basin of attraction of the final critical point. Only $(3,-3)$ points display three-dimensional basins of attraction. In the case of a nuclear maximum, the union of the nuclear point plus its basin of attraction is identified with the concept of atom. When considering a $(3,-1)$ point, the two trajectories originating from it have different nuclear attractors. We then say that those two nuclei are bonded. The presence of a $(3,-1)$ critical point between every pair of bonded nuclei is in agreement with Slater's image of chemical bonding, and we refer the reader to the appropriate literature for further study.[2] The network formed by the nuclei and their bonds is a connected graph, the *molecular graph*. When the molecular graph displays a cycle, the system is said to have a ring. It is found that a ring of bonds is also associated with a $(3,+1)$ point, located somewhere in between the ringed nuclei. Finally, a set of noncoplanar rings may create a cavity holding a cage $(3,+3)$ point in its interior.

This fully coherent picture of the topological structure of a molecular system is to be supplemented with the actual procedures to obtain atomic or group properties. The atomic average value of an observable $\hat{O}$ is defined as the average of the appropriate operator density over the basin of attraction of the atom under consideration,[2]

$$O_\Omega=\langle\hat{O}\rangle_\Omega=\int_\Omega\rho_O dv. \tag{2}$$

The main result that may be proven from the above definition lies in the additivity of atomic properties. The average

TABLE I. Symmetry of fixed point positions that assure the presence of a critical point.

System					
Triclinic	$C_i(\bar{1})$				
Monoclinic	$C_{2h}(2/m)$				
Orthorhombic	$D_2(222)$	$D_{2h}(mmm)$			
Tetragonal	$C_{4h}(4/m)$	$D_4(422)$	$D_{2d}(\bar{4}2m)$	$D_{4h}(4/mmm)$	
Trigonal	$C_{3i}(\bar{3})$	$D_3(32)$	$D_{3d}(\bar{3}m)$		
Hexagonal	$C_{3h}(\bar{6})$	$C_{6h}(6/m)$	$D_6(622)$	$D_{3h}(\bar{6}2m)$	$D_{6h}(6/mmm)$
Cubic	$T(23)$	$T_h(m3)$	$O(432)$	$T_d(\bar{4}3m)$	$O_h(m\bar{3}m)$

value of an observable is given simply by the sum extended over all the three-dimensional attractors of the system of its atomic contributions,

$$\langle \hat{O} \rangle = \sum_{\Omega} O_{\Omega} . \tag{3}$$

This result holds for both one- and two-electron operators. Group properties are immediately obtained after adding the properties of those atoms forming up the group of interest. It is worth mentioning that the virial and other important physical theorems hold within every basin. As it should follow from this enumeration of properties, the partition of space based on Eq. (1) is a fundamental one rather than a computational trick.

Let us finally notice that the molecular graph depends parametrically on the nuclear coordinate variables. As the number of distinct molecular graphs that a particular system may exhibit is finite and discrete, we have essentially obtained a continuous to discrete mapping between the space of nuclear configurations and the space of molecular graphs. The set of points of the nuclear configuration space associated to a given molecular graph is called a *structure*.[9] When the electron density of such a system rearranges as a consequence of external or internal processes, the change of structure must be necessarily catastrophic, in Thom's sense,[10] and it occurs through special degenerate graphs. We then have not only a theory of structure but also of *molecular change*.

B. Ions (atoms) in crystals

1. Basic facts

The periodicity of a crystal lattice is the origin of a set of peculiarities in the topology of the charge density that deserves a more detailed analysis. In the first place, by means of topological identification of equivalent lines and faces in any crystallographic cell, the electron density space domain may be made homeomorphic to S^3, the 3-torus. This fact forces, on the one hand, the finiteness of every atomic basin. In this way, we may assign to every crystalline atom a perfectly defined finite volume. These atomic volumes are additive and fill the space. On the other hand, the existence of $(3,+3)$ critical points or cages, very unusual objects in isolated small molecules, is here assured by the Weierstrass theorem. Moreover, the existence of cage points also enforces the presence of ring points, and the latter, proceeding recursively, that of bond points. All four types of null-gradient points of the electronic density must then be present in a periodic system.

Point-group symmetry has also an important role on the position of the critical points of a scalar function. Let us consider, for example, a pure C_n rotation axis that, without loss of generality, will be supposed along the z axis. The behavior of a scalar function f under the rotation about C_n is such that $f(\vec{h}) = f(R\vec{h})$, where $\vec{h}$ is the position of a point referred to a suitable point of the rotation axis, and

$$R = \begin{pmatrix} \cos\phi & \sin\phi & 0 \\ -\sin\phi & \cos\phi & 0 \\ 0 & 0 & 1 \end{pmatrix} \tag{4}$$

is the rotation matrix of the axis, $\phi = 2\pi/n$ being the rotation angle. For a sufficiently small $\vec{h}$ vector, a first-order Taylor expansion leads to the identity $\nabla f(1-R)\cdot\vec{h} = 0$. If the rotation angle is different from zero, the only nontrivial solution forces the gradient to be along the axis. According to this, any derivative of a scalar function in a direction perpendicular to the rotation axis is null by symmetry at any point along the axis. Similar, very simple arguments indeed, may be applied to the other point-group symmetry elements.

Going further, certain combinations of symmetry elements at a given point assure a null gradient at that point. Table I shows the symmetry of such special positions that *fix a point*. They may be easily obtained for each space group of we realize that they are nothing but those Wyckoff positions having three fixed coordinates. It is also interesting to notice that all other special positions, though not directly ensuring the occurrence of a critical point, limit their possible location strongly. One- and two-parameter special positions may exhibit a null gradient point at selected values of those parameters, though, in many cases, the critical point may coincide with actually fixed positions. Following these prescriptions, a number of symmetry-related points may be found or bracketed by inspection.

Another issue that must be addressed regards topological constraints over the particular number of critical points (CP's) of each kind that may coexist in the lattice. When the domain space of the charge density is R^3, as in an *in vacuo* molecule, the number of CP's must satisfy the Euler or Poincaré-Hopf relation

$$n - b + r - c = 1, \tag{5}$$

where n,b,r, and c refer to the total number of nuclear, bond, ring, and cage points, respectively. In S^3, the 3-torus space of crystal structures, however, the appropriate relations are generally known as Morse relations (see Ref. 11 for a rigorous presentation, or Ref. 12 for a nontechnical discussion). They are well known in solid-state theory since the introduction of van Hove singularities, though its first use in connection with the number of critical points of the electron density in a crystal seems to be that found in Ref. 13. The Morse equivalent to Eq. (5) is

$$n-b+r-c=0, \quad n\geqslant 1, \quad b\geqslant 3, \quad r\geqslant 3, \quad c\geqslant 1. \quad (6)$$

Besides its theoretical importance, Morse relations are extremely useful in order to accept or reject a set of CP's when constructing an automatic search procedure, as we will show below.

Periodicity also has another important consequence that has not yet been recognized. There exists a partition of space into three-dimensional regions surrounded by zero-flux surfaces that is thinner than the partition into atomic basins. Let us define a *primary bundle* as the set of trajectories of the gradient field with common α and ω limits or, in other words, the bundle of trajectories starting at a minimum and ending at a maximum. The boundary surface of a primary bundle is, evidently, a zero-flux surface and, most importantly, the division of space into primary bundles is the thinnest one possible. All CP's must lie on the boundary of a primary bundle. The general structure of a nondegenerate primary bundle is simple. It consists of one maximum, one minimum and, let us say, n ring points and n bond points joined together in a peculiar way: the maximum joins to all the bond points; every bond point joins, moreover, to two ring points; and every ring point joins to the minimum and to two bond points. This scheme induces a homeomorphism between a primary bundle and a convex polyhedron. To each CP we associate a vertex of the polyhedron, and an edge to every trajectory onto the surface of the bundle that connects two CP's. These polyhedra are easily seen to have $2n+2$ vertices, $2n$ faces, and $4n$ edges. They fulfill, thus, Euler relation: faces + vertices = edges $+2$. The most basic topological structure of the crystal is, then, that of its distinct primary bundles, and of their interconnections.

Primary bundles are, however, not found in common topological analyses of the electronic density. They are normally collected to introduce coarser partitions of space in which larger zero-flux-bounded regions are taken as the primary objects of study. The usual practice has been to identify those basic objects as the union of all the primary bundles sharing the same maximum. The interior of such an object is nothing but the basin of attraction of the nucleus. All other critical points of the set of primary bundles defining the atomic basin are found on the surface of the latter, defining another mapping onto sets of polyhedra, the attraction or atomic polyhedra. The mapping is made in the following way: to each cage we associate a vertex of the polyhedron; to each bond point a face that is physically its two-dimensional basin of attraction; and to every ring point an edge that corresponds to its one-dimensional basin of attraction. In this way, an atomic polyhedron with m vertices is composed of m primary bundles.

The recognition of bundles as the intrinsic topological units that form up the crystal allows us to group them together in other ways, giving rise to fruitful, encouraging perspectives of the same realm. One immediate grouping recipe is found by collecting all bundles sharing the same cage to form the topological basic object. This prescription is symmetrical to the previous one with respect to the interchange of basins of attraction by basins of repulsion: the set of points of the space sharing the same α limit. In this way, a repulsion polyhedra has a minimum in its interior. In its surface, nuclei define vertices; ring points and their two-dimensional repulsion basins define faces; and bond points and their one-dimensional repulsion basins define edges.

Once attraction and repulsion basins and polyhedra have been introduced, a very clear chemical image appears. To every atomic species in the crystal we associate an attraction or atomic polyhedron with as many faces as different bonds attached to the atom considered, giving rise to a continuous to discrete mapping between the set of possible nuclear configurations and the set of topological polyhedra. Attraction polyhedra are then to be interpreted as atomic shapes. On the other hand, repulsion polyhedra are directly associated to the bonding network of the structure, having vertices along bond lines. Both visions complement each other. The objective definition of the number of bonds attached to a given atom that originates in the above arguments allows us to define unambiguously concepts as important to solid state physics and chemistry as the coordination index of an atom and its associated coordination polyhedron. In this sense, classification schemes based upon such definitions acquire a well-founded status.

Primary bundles, finally, can be gathered together to form the topological equivalent to the Wigner-Seitz cell of the crystal, recently introduced by Zou and Bader[6] as the smallest connected region of space bounded by a zero-flux surface, and exhibiting the translational and local point-group invariance of the crystal. Actual atomic or repulsion polyhedra are difficult to visualize, as their computation implies expensive calculations. The mapping among them and polyhedra, however, opens the question about the possibility of finding planar polyhedra that approximate the actual shape of the topological polyhedra. It is easy to understand, for example, that the proximity polyhedron of an atom is a first-order approximation of its atomic basin. A proximity polyderon is defined as the region formed by the intersection of the set of semispaces that contain the nucleus of interest, generated by all the planes that perpendicularly bisect the lines connecting the nucleus with its neighbors; or, in other words, as the Wigner-Seitz cell of a hypothetical Bravais lattice containing one node at each nuclear position.

Proximity polyhedra (PP) of different atoms display the full local point-group symmetry at the nuclear sites, share faces when considering neighboring nuclei, and fill the space without overlapping. These features are also characteristic of atomic basins, as commented above. It is easily proven that they are actually the atomic basins when the atoms of the lattice are all equal (i.e., in the case of metals). If there exist different species, however, different coordination indices may appear, and the PP associated to each kind of atom will have to be obtained with respect to the coordination actually exhibited and the relative distance from every bonded neigh-

bor at which the bisecting planes are drawn. We name the PP's in this case as *weighted proximity polyhedra* (WPP's). Moreover, the atomic basins of the larger atoms will expand with respect to their WPP's, while the basins of the smaller will shrink. Along with this process, the planar faces of the WPP may distort, and bumps appear. We will show that, actually, there exist crystals with mostly planar atomic faces and crystals with striking features in their atomic shapes. In any case, PP's play an important role in the intuitive understanding of atomic shapes.

From the topological polyhedra just defined, new illuminating three-dimensional objects may be obtained by means of the concept of Euclidean or geometrical duals. Given a polyhedron, another (its dual) is constructed associating to each of its faces a vertex, and vice versa. Two vertices of this other polyhedron are joined by an edge if the corresponding faces in the original figure are adjacent. Two kinds of polyhedra arise using this prescription. In order to keep the discussion as succinct as possible, we will only briefly consider the duals of the attraction polyhedra. They must have a vertex per bond attached to the atom under consideration. If we locate these vertices at the nuclear position of the bonded atoms, we obtain a procedure to obtain the coordination polyhedron of any atomic species. Sixfold coordination, for example, conduces to octahedralike coordination polyhedra (six corners, eight faces, 12 edges) and to cubelike atomic shape polyhedra (eight corners, six faces, 12 edges). It is also interesting to note that when a change in the structure or in the electronic density leads to a change in the number or type of the CP's of the system, all the polyhedra here defined must undergo a similar change of type simultaneously.

2. Automatic search of critical points

From the above considerations, it stands clear that the topological structure of a modest mineralogical compound is expected to be rather complex. If our aim is to analyze the whole topology of the crystal, rather than studying a particular topological feature, we need an efficient method of finding all CP's.

We will start by assuming that input electron densities have been obtained by means of any suitable procedure (i.e., some kind of *ab initio* calculations, or even high precision experimental data, see Ref. 14 for an interesting review on recent advances in this field). We will also assume that first- and second-order spatial derivatives of the charge density may be obtained to a given desired accurary. The means to accomplish this task will vary according to the source of the data. Nuclear positions, as well as the crystal space group, will be also supposed to be given.

Our procedure tries to reduce as much as possible the size of the search space. To do that, we first construct the Voronoi polyhedron of the Bravais lattice by means of Finney's algorithm.[15] Using symmetry information, it is compacted to its irreducible wedge, or irreducible Wigner–Seitz zone (IWZ). The IWZ is composed of one (or a small number at worst) of irreducible tetrahedra (IWT). When there is more than one, the IWT's share vertices, edges, and faces, and may be fused together to form an unique IWZ, or else they may be left separated while keeping track of duplicate points. All nonequivalent special positions in the unit cell are found on the surface of the IWZ (or IWT's). Fixed points, or symmetry fixed CP's, coincide with the vertices of the IWZ; one- and two-parameter special points, with its edges and faces. Finally, Wyckoff's general positions of the lattice will be located in the inside of the IWZ.

Our algorithm proceeds as follows. We locate, as a first step, all nuclear and symmetry-fixed CP's by examining the input crystallographic positions and the vertices of the IWTs. The algorithm then looks for a CP of the charge density in a given l simplex (segment, triangle, or tetrahedron when $l=1$, 2, or 3). A rather safe way to locate the CP is to search for a minimum of $|\nabla\rho|$ using a good multidimensional minimization scheme (like linear downhill simplex or Powell's method[16]), and to check if this minimum achieves a null gradient to a required precision. We then proceed by applying a slightly modified baricentric subdivision algorithm to each of the l simplices. A tree data structure is created containing one node per each simplex within a given IWT (4 corners + 6 edges + 4 faces + 1 tetrahedron= 15 nodes). The previously commented minimization routine is then used to select one CP out of all the possible ones lying in the interior of the simplex associated to every node of the tree. If another CP is found, a division of that simplex is done. The division position is taken as the location of the CP just found, rather than as a geometric center of the simplex. The division is recursively repeated until no CP is found at a particular tree node. In this case, the node is end marked, and the algorithm proceeds with another node until all of them have been end marked. Clearly, the method is finite and exhausts all possible CP's. In order to avoid infinite loops due to numerical inaccuracies, however, a maximum tree depth is enforced, so finiteness is guaranteed.

The above scheme has been implemented in a FORTRAN 77 (Ref. 17) code that receives externally computed charge densities and searches for the topological structure of the CP's in a crystal. At present, densities are supposed to be obtained through *ab initio* perturbed ion,[18–20] calculations. The code also contains a post-search analysis of the CP's, that includes a Morse consistency test, a study of bonding relations in the case of bond points, and a symmetry classification of any of the CP's found. With the help of this method, systematic investigations of both structural and energetic relations in crystal families are made feasible.

III. APPLICATION: *B*1 PHASE OF THE LiI CRYSTAL

We describe in this section how the general procedures previously devised are particularized for a prototype system, in this case the B1 phase of LiI. We will first briefly comment upon the computational scheme used to obtain the electron density.

A. Computational scheme

Ionic crystals, or generally, closed-shell interacting systems, are characterized by displaying a large number of possible crystal structures, from the very simple to the very complex ones. In every case, charge density is expelled out of bonding (interatomic) regions and accumulates in the ionic cores. As a consequence, all topological features except nuclear maxima positions are found at extremely low-density locations. Well-resolved densities are then needed to isolate and relate all the independent CP's successfully. Along this

TABLE II. Special positions (in Wyckoff's notation) for the $Fm3m$ group.

Multiplicity	Wyckoff letter	Symmetry	Representant
192	l	C_1	(x,y,z)
96	k	C_s	(x,x,z)
96	j	C_s	$(0,y,z)$
48	i	C_{2v}	$(\frac{1}{2},y,y)$
48	h	C_{2v}	$(0,y,y)$
48	g	C_{2v}	$(x,\frac{1}{4},\frac{1}{4})$
32	f	C_{3v}	(x,x,x)
24	e	C_{4v}	$(x,0,0)$
24	d	D_{2h}	$(0,\frac{1}{4},\frac{1}{4})$
8	c	T_d	$(\frac{1}{4},\frac{1}{4},\frac{1}{4})$
4	b	O_h	$(\frac{1}{2},\frac{1}{2},\frac{1}{2})$
4	a	O_h	$(0,0,0)$

line, we have chosen (as in our previous works) the *ab initio* perturbed ion method *ai*PI,[18–20] a quantum-mechanical scheme extensively tested in several groups of ionic and partially ionic solids. In brief, the method solves the Hartree-Fock (HF) equations of the solid in a localized Fock space. Many of the advantages of this scheme over canonical approaches emanate from the localizing procedure. On the one hand, it allows us to use large, nearly HF basis sets to avoid balancing problems. We have used here the multi-ζ exponential basis sets of Clementi and Roetti.[21] On the other hand, the resulting local wave functions are very well suited to obtain good (perturbativelike) estimations of the correlation energy correction to the HF energy.[22]

The electronic densities and crystal geometries that are taken as input in the topological analysis have been obtained by minimizing the electronic ground-state potential surface with respect to the only structural parameter characterizing the $B1$ phase of LiI, the a lattice parameter. The theoretical values obtained for a, the cohesive energy, and the isothermal zero-pressure bulk modulus (B_0) are 4.359 Å, 728.0 kJ/mol, and 16.58 GPa, respectively, to be compared with the experimental room temperature data, 4.259 Å, 763.6 kJ/mol, and 17.17 GPa.[23] We will use only equilibrium theoretical results in what follows.

B. Topology

LiI crystallizes, at low temperatures and pressures, in the rocksalt phase, space group $Fm3m$. A summary of the Wyckoff special positions for this group is shown in Table II. Let us notice that there are four different fixed points. Two of them are occupied by the lithium (say position $4a$) and the iodine ($4b$) nuclei. It follows from the previous considerations that the two other fixed locations ($8c$ and $24d$) must be true CP's of the structure.

From Table II, it also becomes clear that all the relevant special positions in the crystal are contained in two selected planes: [100] and [110], for example. Contour density plots of the charge density on both planes are shown in Fig. 1. It should be taken into account that the density scale is logarithmic, and that the CP's found by the automatic algorithm, as well as the zero-flux surfaces projections, are superimposed at the appropriate locations. Let us examine in detail several interesting facts that emerge from the figures.

In the first place, both the lithium and iodide ions are remarkably spherical. If we remember that non-nuclear CP's lie on the atomic surfaces, we observe that the lithium cation shows a rather constant nucleus-CP distance (radius) along different directions. Conversely, the iodide anion shows small but significative deviations from sphericity, mainly along the anion-anion contact direction. It is particularly clear from Fig. 1(b) that the iodides can be seen as forming a cubic close-packed structure in which the octahedral holes are filled by the smaller lithium ions. This allows us to define an iodine radius from the a lattice parameters, as has been repeatedly suggested in the literature.[25] The strong anion-anion contact shown here has important consequences on the stability and cohesive energy of the $B1$ phases of the alkali halides, as we are going to discuss in depth in a subsequent paper.

In the second place, the charge-density plots show how almost all the interatomic lines and surfaces deviate very slightly from linearity or planarity, respectively. This means that the atomic surface will be very well approximated by the WPP of the atom considered. Moreover, when bumps appear in the surfaces, it is the lithium which expands against the iodide. This fact is also consistent with our chemical intuition that regards the large halide anions as much more deformable (or polarizable) entities than the small alkali cations.

In order to obtain all the CP's and their exact location, the automatic search code shows that the irreducible Wigner-Seitz zone contains only one irreducible tetrahedra, being the vertices: $(0,0,0)$, $(\frac{1}{2},0,0)$, $(\frac{1}{4},0,\frac{1}{4})$, and $(\frac{1}{4},\frac{1}{4},\frac{1}{4})$, for example. Its four corners are then, according to Table I, the four symmetry-fixed CP's. Only four independent CP's are found by the baricentric process. There are two different independent CP's for each of the four possible classes: nuclear, bond, ring, and cage points. On the whole, a primitive LiI cell contains two nuclear points, 12 $(6+6)$ bond points, 20 $(12+8)$ ring points, and 10 $(2+8)$ cage points. As can be immediately proved, these numbers fulfill the Morse relations, and constitute, therefore, a consistent set of CP's for the crystal. Table III shows the specific positions, densities, and computed gradient modules for all of them. First, it is important to notice that the charge densities vary eight orders of magnitude from the value found at the iodide nucleus to that at the $8c$ cage, the absolute density minimum. Second, by means of the automatic determination as well as by visual inspection, the two bond points are found to bond different pairs of atoms. CP number 3 ($24e$) is a Li-I bond, while symmetry-fixed CP number 4 ($24d$) is a I-I bond. No Li–Li bond exists, meaning that the lithium has a sixfold coordination, and the iodine a 18-fold (sixfold + 12-fold) one. While this is in contrast with traditional thinking, it is our opininon that we should retain the topological 6-18 structure. We must remark that, although the $24d$ point is necessarily a CP in every alkali halide, by no means it is required to be a bond point and, in fact, it is not in many alkali halides.

It is immediate to obtain the bonded radii of each ion from Table III: 0.9377 Å for the lithium, and 2.1448 or 2.1797 Å for the iodine along the I-I and I-Li directions, respectively. These values are in good agreement with Shan-

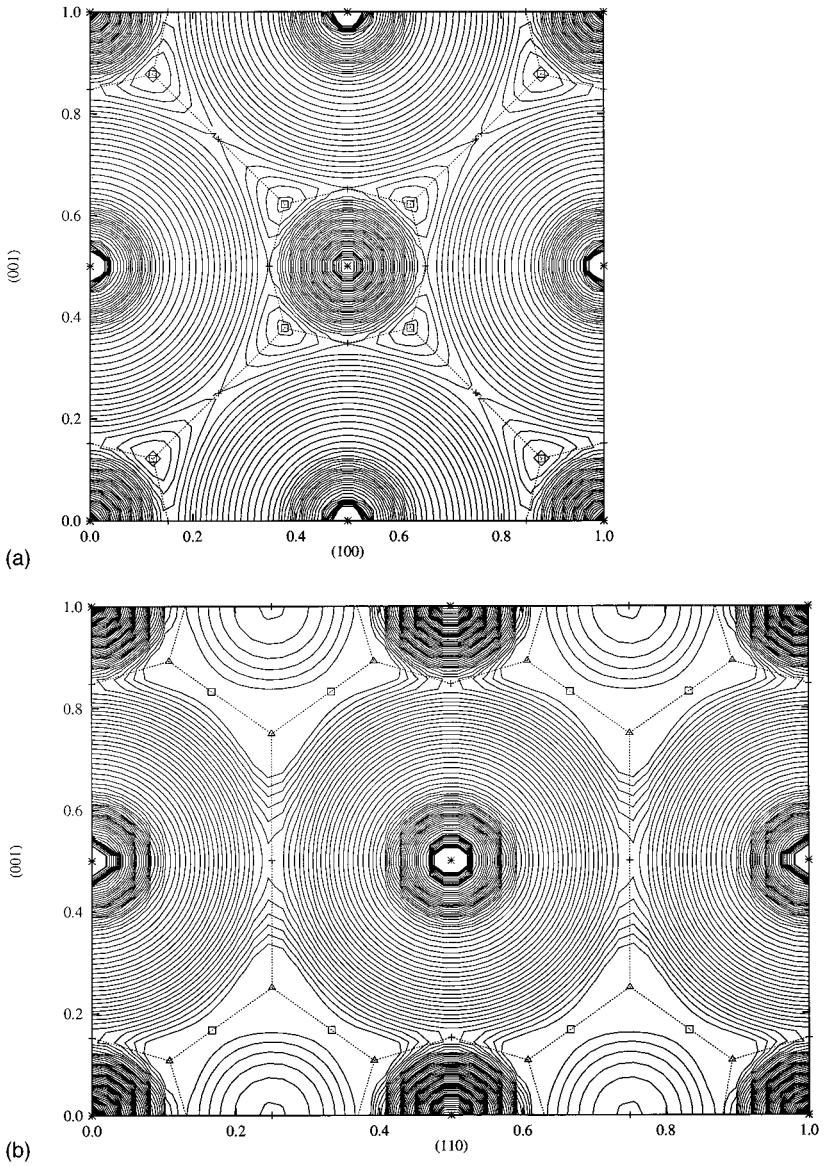

FIG. 1. Contour density plots of the charge density scalar field in the LiI $B1$ crystal at its theoretical equilibrium lattice parameter. lithium is at (0,0,0), and iodine at $(\frac{1}{2},0,0)$. (a) Density on the [100] plane. (b) Density on the [110] plane. The isolines scale is logarithmic, in such a way that there are 50 contours between the absolute minimum and the absolute maximum. Critical points and zero-flux surfaces limits have been superimposed with the following conventions: dotted lines for surface limits, stars for nuclear points, crosses for bond points, squares for ring points, and triangles for cage points. The axes labels stand for the appropriate crystallographic direction, and the units used are also crystallographic.

non and Prewitt's radii, 0.9 and 2.06 Å,[24] or with the theoretical values given by Adachi,[25] 0.95 and 2.07 Å . We emphasize that these data have been fully obtained from an *ab initio* point of view, and that the a lattice parameter has not been fixed to the experimental value, as has been usual practice in previous investigations.[25]

Further insight concerning the spatial organization of CP's may be obtained by following three different paths. In the first one, we examine the atomic attraction polyhedron of each ion to obtain a clear picture of the vertex-edge-face relation previously defined. In the second one, the geometrical arrangement of CP's relative to the repulsion polyhedron

TABLE III. LiI independent critical points. Positions in crystallographic units. Electronic densities and gradients in atomic units. The symbols n, b, r, and c refer to nuclear, bond, ring, and cage points, respectively.

Number	Symmetry	Type	Representant	ρ	$\lvert\nabla\rho\rvert$
1	4a	n	(0.000 00, 0.000 00, 0.000 00)	1.3722×10^{2}	
2	4b	n	(0.500 00, 0.000 00, 0.000 00)	1.0503×10^{5}	
3	24e	b	(0.152 10, 0.000 00, 0.000 00)	4.4858×10^{-3}	3.5×10^{-8}
4	24d	b	(0.250 00, 0.000 00, 0.250 00)	5.5567×10^{-3}	2.1×10^{-11}
5	48h	r	(0.122 10, 0.000 00, 0.122 10)	2.3112×10^{-3}	1.1×10^{-8}
6	32f	r	(0.166 92, 0.166 92, 0.166 92)	2.1400×10^{-3}	1.0×10^{-8}
7	32f	c	(0.107 31, 0.107 31, 0.107 31)	1.6903×10^{-3}	4.1×10^{-8}
8	8c	c	(0.250 00, 0.250 00, 0.250 00)	1.4466×10^{-3}	1.4×10^{-12}

TABLE IV. Trace ($\nabla^2\rho$), eigenvalues (ϵ_i), and normalized eigenvectors (V_x, V_y, V_z) of the Hessian matrix of the charge density at non-nuclear critical points. All density data in atomic units.

Number	$b3$	$b4$	$r5$	$r6$	$c7$	$c8$
$\nabla^2\rho$	0.032 77	0.014 85	0.044 72	0.008 03	0.009 69	0.006 32
ϵ_1	−0.004 73	−0.026 95	−0.001 58	−0.000 98	0.002 78	0.002 11
V_x	0.000 00	0.000 00	1.000 00	−0.577 35	0.408 25	0.577 35
V_y	0.707 11	0.707 11	0.000 00	−0.577 35	0.408 25	0.577 35
V_z	0.707 11	−0.707 11	0.000 00	0.577 35	0.816 50	0.577 35
ϵ_2	−0.004 73	−0.002 69	0.005 57	0.004 51	0.002 78	0.002 11
V_x	0.000 00	1.000 00	0.000 00	0.408 25	−0.707 11	0.707 11
V_y	−0.707 11	0.000 00	0.707 11	0.408 25	0.707 11	−0.707 11
V_z	0.707 11	0.000 00	0.707 11	0.816 50	0.000 00	0.000 00
ϵ_3	0.042 23	0.014 79	0.014 79	0.004 51	0.004 12	0.002 11
V_x	1.000 00	0.000 00	0.000 00	−0.707 11	−0.577 35	0.408 25
V_y	0.000 00	0.707 11	−0.707 11	0.707 11	−0.577 35	0.408 25
V_z	0.000 00	0.707 11	0.707 11	0.000 00	0.577 35	−0.816 50

around each cage is studied. In the third one, the geometrical structure of CP's around each nonequivalent CP is analyzed. All of these approaches are complementary, and need information about the basins of attraction and repulsion of CP's. As far as this last point is concerned, Table IV shows the eigenvalues and eigenvectors of the Hessian of the charge density, $H(\rho)$, at each of the non-nuclear CP's of the crystal. We see, for example, that the basin of CP number 3 (a Li-I bond) is parallel to the yz plane in the proximities of the bond. The bonding direction is simply the x axis and, therefore, the bond angle is 180°. Reasoning in a similar manner for the six bonds around a lithium atom [see the central atom in Fig. 1(a)], we can use intuition to obtain its WPP, that turns out to be a slightly bumped regular cube. It is easily verified that the cage $c7$ forms the eight vertices of the cube, and that there is a ring $r5$ at the very center of each of the 12 edges. The edges of the cube, viewed from its center, are straight lines parallel to the Cartesian axes (see the eigenvector associated to the negative eigenvalue at the $r5$ point in Table IV) that curve slightly inwards near the vertices. We can convince ourselves of the truth of the last statement considering the (0,0,0) lithium in the left-bottom part of Fig. 1(a). The nearest ring point, at (0.1221,0,0.1221), is at the center of an edge along the y axis, and this edge ends at two cage points, situated above the figure's plane at (0.1073,0.1073,0.1073) and (0.107 31, −0.107 31, 0.107 31). The cages are, actually, nearer to the yz plane than the rings. Similar arguments can be easily extended to the iodine atom. In this case, square faces are associated to each one of the six Li-I bonds along the (100) lines, and perfectly hexagonal faces to the 12 I-I (110) bonds. Figure 2(a) displays the ideal (planar faces) WPP's for both atoms, showing their mutual relation and the space-filling property. Figure 2(b) presents the atomic basins obtained from the actual wave function of the crystal. Let us notice the great size difference between the iodine and the lithium atoms. It can be observed that the WPP's are, in this case, a very good approximation to the atomic basins. The duals of this attraction polyhedra (the coordination polyhedra) are now easy to find, and are shown in Fig. 3. The 18-fold coordination of the iodines yields the truncated cube shown, while the sixfold bonding of the lithiums produces a much more familiar regular octahedron.

If the repulsion polyhedron, and not the WPP, is chosen as the root node of the analysis of the arrangement of CP's in the crystal, spatial relations among them appear. From Table III, we see that there are two independent cage points: $7c$ and $8c$. We can use Fig. 2 to visualize its situation. The repulsion polyhedron of CP $7c$ is, for example, the triangular pyramid formed up by the central lithium atom and thea three anions located at $(1,\frac{1}{2},\frac{1}{2})$,$(\frac{1}{2},1,\frac{1}{2})$, and $(\frac{1}{2},\frac{1}{2},1)$. The $7c$ point is situated along the height line of the pyramid at 0.0594 crystallographic units from the base. It is easily verified that the four faces of the pyramid are actually triangular rings of bonds, and that all the edges (or bond paths) are linear (they are symmetry lines). No bent bond stress then arises. The faces are not all planar by symmetry, however, and the base of the pyramid is slightly bumped. Its ring point ($r6$) has a free parameter along one diagonal of the cubic unit cell. Were the base face of the pyramid absolutely planar, it would be situated at $(\frac{2}{3},\frac{2}{3},\frac{2}{3})$. Actually, its position is (0.6669,0.6669,0.6669), only 2.5×10^{-4} crystallographic units away from its ideal location. Ring stress is then negligible for this crystal. The other cage, $8c$—a fixed point with T_d symmetry—lies at the center of the regular tetrahedron formed by the four anions of any of the eight little cubes forming the cubic unit cell. Its four faces are equivalent equilateral triangles of anion-anion bonds. The bonds network in this crystal is then a union of three-member rings of bonds (some isosceles triangles, some equilateral ones) surrounding tetrahedral or pyramidal cages. Let us notice that the cage points of the crystal may be correlated with the concept of *holes* of a structure, the points inside a crystal where a host ion or impurity is most likely to be found.

Finally, some information may be gained by examining the distribution of CP's around every CP. When applied to nuclear positions, it gives rise to the shell structure of the crystal, or to the radial distribution function of neighbors,

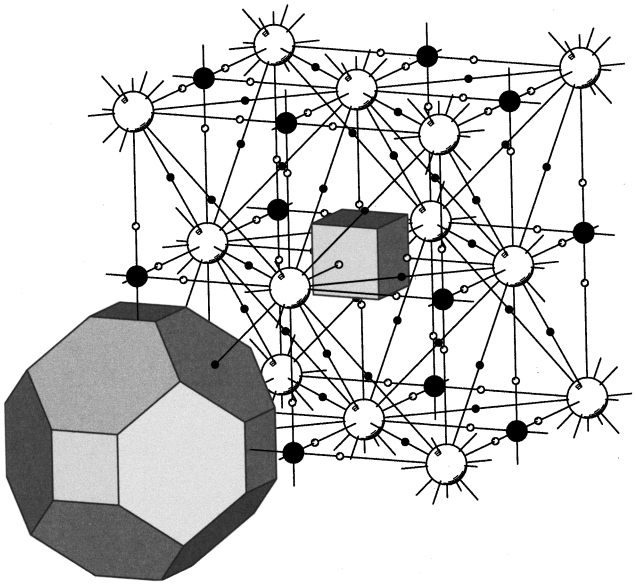

(a)

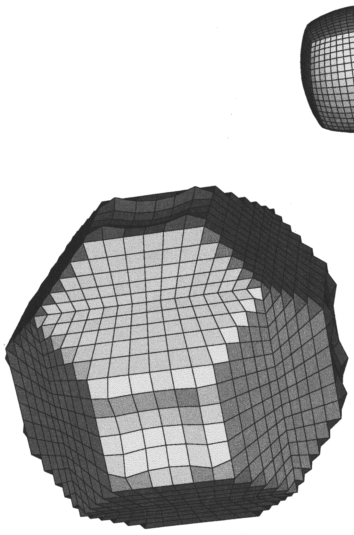

(b)

FIG. 2. (a) Weighted proximity polyhedra for the LiI structure onto the cubic unit cell. Lines correspond to Li-I and I-I bonds. Filled small dots correspond to I-I bond points, and hollow small dots to Li-I ones. In order to allow for a better view, the relative position of cations and anions has been inverted with respect to Fig. 1. Large white spheres are iodide ions, and large black spheres lithium cations. Note the space-filling property of the polyhedra. (b) Attraction basins of I (left) and Li (right). The basins have been rendered with GEOMVIEW (Ref. 27).

both extensively studied in the past. We will briefly describe, therefore, the shell structure of non-nuclear CP's, and the non-nuclear neighbors of nuclear points. It is easy to visualize the geometry of CP's around a given one by using Fig. 2. For example, if we take the $c8$ point (the *tetrahedral hole* of the NaCl structure), the first neighbors are the four centers of the faces of its repulsion tetrahedron, followed by the four cages of the other kind situated tetrahedrically around it in the interior of the four pyramids, and by the six I-I bonds at

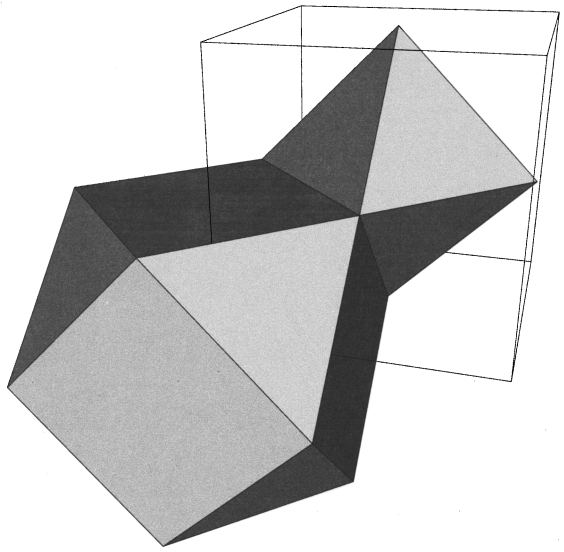

FIG. 3. Coordination polyhedra for the LiI structure onto the cubic unit cell. Atomic positions are equivalent to those of Fig. 2. Note that now the polyhedra interpose each other.

the centers of the edges forming its repulsion tetrahedron. We must also stress the great density of CP's in a crystal and their mutual proximity. In the case under study, the minimum distance between two different CP's is 0.63 Å in the $r6$-$c7$ case, which is a very small value and contributes to the intrinsic algorithmic difficulty of automatically finding all CP's. Even more illuminating about the CP proximity is the fact that in the list of neighbors of the $b3$ bond point, the iodine nucleus is not among the first 20 neighbor shells around it.

C. Atomic properties

We will now present a very brief account of the results obtained when integrating some operators over the basin of attraction of an atom. A recent account of the basic theoretical facts concerning these properties is given in Ref. 26. We will restrict ourselves here to the atomic charge and to the atomic volume of the two species in the LiI crystal and defer further considerations to other papers in this series.

The computational code we have constructed obtains automatically the atomic values of several operators by means of a three-dimensional Gauss-Legendre numerical quadrature performed in a polar coordinate frame centered at each nonequivalent nuclear position in the crystal. The most difficult part of the radial integration is the calculation of the boundary of the atomic basin at each value of the polar angles and it constitutes the limiting step of the algorithm. Convergence tests are done by examining the total charge of the unit cell, the total volume as compared to the crystallographical one, and the value of the integral of the Laplacian of the charge density over atomic basins. This last value should ideally be zero by transforming the volume integral to a surface one. We have found total cell residual charge values around 10^{-4}–10^{-5} electrons as typical of usual integration grids. Symmetry is presently accounted for by directly introducing the integration limits, but will be soon incorporated to integrate automatically over the irreducible region of each atomic basin.

Using a quadrature of $70\times70\times70$ points we have obtained the following values: $Q_{Li}=-Q_I=0.970\,13$ a.u., $V_{Li}=29.6191$ bohr^3 (7.496% of total), and $V_I=365.5213$ bohr^3 (92.504% of total). These values, situate the LiI as a highly ionic compound, and allows us to speak with confidence of *ions in a crystal*.

IV. CONCLUSIONS

We have shown in this paper how Bader's theory of atoms in molecules may be applied to periodic crystalline systems. Some specific facts emerging from the topological difference between R^3, the three-dimensional space of isolated molecules, and S^3, the three-dimensional manifold of a crystal, have been studied in detail. Symmetry has been shown to impose stringent conditions on the location of critical points of the charge-density gradient field. An automatic algorithm for the location and analysis of critical points has been constructed and used to exemplify the theoretical results. We have also shown how the topology of the electron density may be used to give a rigorous foundation to historical concepts like the index of coordination or the coordination polyhedron of an atom or ion in a solid. Several interesting mappings between atoms and polyhedra have also been examined, and applied to a LiI system. We think that there is room in solid-state thinking for the tools and concepts presented here, and that a judicious use of them will give rise to ways of correlating chemical behavior and chemical structure in solids. An attempt to present some of those findings will be the purpose of the following parts of this work.

ACKNOWLEDGMENTS

We are grateful to the Centro de Cálculo Científico of the Universidad de Oviedo for computational facilities. Financial support from the Spanish Dirección General de Investigación Científica y Técnica (DGICYT), Project No. PB93-0327, is also acknowledged.

[1] P. G. Mezey, Theoret. Chim. Acta (Berlin) **54**, 95 (1980); **58**, 309 (1981); **60**, 409 (1982); **63**, 9 (1983); P. G. Mezey, J. Chem. Phys. **78**, 6182 (1983); G. A. Arteca and P. G. Mezey, *ibid.* **93**, 4746 (1989); J. Pospíchal, and V. Kvasnička, Theoret. Chim. Acta **76**, 423 (1990); M. Rèrat, D. Liotard, and J. M. Robine, *ibid.* **88**, 285 (1994), and references therein.

[2] R. F. W. Bader, *Atoms in Molecules* (Oxford University Press, Oxford, 1990).

[3] R. J. Gillespie, *Molecular Geometry* (Van Nostrand Reinhold, London, 1972).

[4] R. F. W. Bader, Can. J. Chem. **64**, 64 (1986).

[5] M. E. Eberhart, M. M Donovan, and R. A. Outlaw, Phys. Rev. B **46**, 12 744 (1992); M. E. Eberhart, D. P Clougherty, and J. M. MacLaren, J. Mater. Res. **8**, 438 (1993).

[6] P. F. Zou and R. F. W. Bader, Acta Crystallogr. A **50**, 714 (1994); V. G. Tsirelson, P. F. Zou, T. Tang, and R. F. W. Bader, *ibid.* A **51**, 143 (1995).

[7] A. Martín Pendás, V. Luaña, J. M. Recio, M. Flórez, E. Francisco, M. A. Blanco, and L. N. Kantorivch, Phys. Rev. B **49**, 3066 (1994)

[8] R. F. W. Bader, Chem. Rev. **91**, 893 (1991).

[9] R. F. W. Bader, T. T. Nguyen-Dang, and Y. Tal, J. Chem. Phys. **70**, 4316 (1979); R. F. W. Bader, T. T. Nguyen-Dang, and Y. Tal, Rep. Prog. Phys. **44**, 893 (1981).

[10] R. Thom, *Structural Stability and Morphogenesis* (Benjamin, Reading, MA, 1975); K. Collard and G. G. Hall, Int. J. Quantum Chem. **12**, 623 (1977).

[11] M. Morse and S. S. Cairns, *Critical Point Theory in Global Analysis and Differential Geometry* (Academic, New York, 1969).

[12] W. Jones and N. H. March, *Theoretical Solid State Physics* (Dover, New York 1985), Vol. 1, App. A1.6.

[13] C. K. Johnson (unpublished).

[14] P. Coppens, Ann. Rev. Phys. Chem. **43**, 663 (1992).

[15] J. O'Rourke, *Computational Geometry in C* (Cambridge University Press, Cambridge 1994).

[16] W. H. Press, B. P. Flannery, S. A. Teukolsky, and W. T. Vetterling, *Numerical Recipes* (Cambridge University Press, New York, 1986).

[17] The code is available from the authors upon request. Contact A. Martín Pendás, electronic address: angel@fluor.quimica.uniovi.es

[18] V. Luaña and L. Pueyo, Phys. Rev. B **41**, 3800 (1990).

[19] V. Luaña, A. Martín Pendás, J. M. Recio, E. Francisco, and M. Bermejo, Comput. Phys. Commun. **77**, 107 (1993).

[20] J. M. Recio, A. Martín Pendás, E. Francisco, M. Flórez, and V. Luaña, Phys. Rev. B **48**, 5891 (1993), and references therein.

[21] E. Clementi and C. Roetti, At. Data Nucl. Data Tables **14**, 177 (1974).

[22] S. J. Chakravorty and E. Clementi, Phys. Rev. A **39**, 2290 (1989).

[23] *Handbook of Chemistry and Physics*, 64th ed., edited by R. C. Weast (Chemical Rubber Co., Boca Raton, FL, 1983).

[24] R. D. Shannon and C.T. Prewitt, Acta Crystallogr. B **25**, 925 (1965).

[25] H. Adachi, J. Phys. Soc. Jpn. **62**, 3965 (1993).

[26] R. F. W. Bader, Phys. Rev. B **49**, 13 348 (1994)

[27] M. Phillips, T. Munzner, and S. Levy, GEOMVIEW, available via anonymous ftp from geom.umn.edu (The Geometry Center at the University of Minnesota).